CONF-771120--16

ANALYTICAL DESCRIPTION OF THE EFFECTS OF MELTING PRACTICE AND HEAT TREATMENT ON THE CREEP PROPERTIES OF 2 1/4 Cr-1 Mo STEEL*

M. K. Booker

Metals and Ceramics Division
Oak Ridge National Laboratory
Oak Ridge, Tennessee 37830

ABSTRACT

2 1/4 Cr-1 Mo steel is used worldwide as an elevated-temperature structural material, particularly in steam generation systems. Since this material is often used at service temperatures up to 600°C, successful design requires a consideration of its creep properties. Unfortunately, the development of an analytical description of the creep behavior of 2 1/4 Cr-1 Mo steel is complicated by two phenomena. First, the creep strength of this material is quite sensitive to heat treatment. Second, this material tends to exhibit nonclassical creep under some conditions. In addition, especially in nuclear applications, the material used may be air-melted, vacuum-arc remelted (VAR), or electroslag remelted (ESR).

In the current investigation, available creep data from air-melted, VAR, and ESR material have been analyzed. Heat treatments included both annealed and isothermally annealed, with and without a subsequent "postweld" heat treatment. It has been found that the elevated-temperature ultimate tensile strength (UTS) is a useful indicator of creep strength for a given heat of material regardless of melting practice or heat treatment. Meanwhile, the nonclassical creep behavior has been attributed to a change in creep mechanism which has been mathematically modeled.

*Research sponsored by the Energy Research and Development Administration under contract with the Union Carbide Corporation.

ANALYTICAL DESCRIPTION OF THE EFFECTS OF MELTING PRACTICE AND HEAT TREATMENT ON THE CREEP PROPERTIES OF 2 1/4 Cr-1 Mo STEEL*

M. K. Booker

The low alloy ferritic 2 1/4 Cr-1 Mo steel has gained worldwide importance as a structural material for elevated-temperature applications in steam generation systems. In particular, the material will be used in the Clinch River Breeder Reactor Plant (CRBRP) steam generators in the air-melted, vacuum-arc remelted (VAR), and electroslag remelted (ESR) conditions. Material used will primarily be annealed or isothermally annealed, with some components receiving an additional postweld heat treatment (PWHT).

The allowable stress values and isochronous stress-strain curves in ASME Code Case 1592 [1] for this material are based on data for air-melted material in the annealed condition. The CRBRP design, then, requires a consideration of the effects of melting practice and of postweld heat treatment on the properties of 2 1/4 Cr-1 Mo steel. In the current investigation, constant-load isothermal creep strain-time data have been analyzed over a range of stresses and temperatures to yield expressions for creep-rupture life, time to tertiary creep, and creep strain-time behavior as functions of time, stress, and temperature. Data came from air-melted, VAR, and ESR material in the annealed and isothermally annealed conditions, with and without postweld heat treatment. A consideration of the phenomenological behavior of this material allowed the development of a creep strain-time equation that can describe the nonclassical creep behavior common to this material. In addition, the equations contain terms involving elevated-temperature ultimate tensile strength. These terms greatly decrease the uncertainty in predictions caused by the large variations in the creep properties of 2 1/4 Cr-1 Mo steel due to heat treatment and heat-to-heat effects. The equation described here is currently recommended for use in the design of the steam generators for the CRBRP.

DATA

The data used in this analysis came from two basic sources: ORNL [2,3,4] data for air-melted material and GE [5,6] data for vacuum-arc remelted (VAR) and electroslag remelted (ESR) material. Tables I and II summarize the heats of material and heat treatments used. Heat treatments included anneal and isothermal anneal, with and without postweld heat treatment for 4 hr at 727°C (1340°F). So we could factor ultimate tensile strength into the creep models, only creep data for heats and heat treatments for which tensile data were also available were used. This restriction forced exclusion of eight GE tests with 40 hr postweld heat treatments (heat treatment ISP1). Overall, data were available from 454 to 566°C (850-1050°F) with test times extending just beyond 12,000 hr. Figure 1 shows the distribution of data in terms of test duration and temperature (earlier data generated by Babcock and Wilcox Corp. were excluded as being of insufficient precision for the current applications).

FEATURES OF EXPERIMENTAL CREEP CURVES

The creep strain-time behavior of 2 1/4 Cr-1 Mo steel can be phenomenologically quite complicated. This material strongly tends toward nonclassical creep behavior. Figure 2 compares a typical nonclassical creep curve exhibited by this material with a classically shaped curve. This behavior is discussed in more detail by Klueh, [2,3,4] who points out that the concave upward portion at the end of the first steady-state stage does not represent the onset of tertiary creep (as one might wrongly be led to believe). Rather, it probably represents a metallurgical instability within the material. The creep rate is controlled by different mechanisms in the two steady-state stages.

The existence of two separate steady-state stages appears to be a dominant feature of the behavior of this material and should be accounted for by any analytical model. For the nonclassical curve shown in Fig. 2, we will call the first primary and steady-state portions "Type I" creep, and the second linear portion "Type II" creep. The stress-temperature conditions under which one sees classical or nonclassical creep vary with heat and heat treatment.

If, as explained above, one wrongly denotes the transition from Type I to Type II creep as the onset of tertiary creep, 2 1/4 Cr-1 Mo steel appears to display very early onset of tertiary creep. For the classical curves available, however, the time to the onset of tertiary creep, t_3, is always about half the rupture life, t_r [2,3]. For the nonclassical curves, the end of the second linear stage is also about half the rupture life. For this reason, it is thought that the "true onset of tertiary creep" is given by the end of this second linear stage. The end of the first linear stage, t_I, represents merely a mechanism change. Figure 3 illustrates this behavior for the ORNL data from air-melted material of Klueh [2,3,4] and typical GE [5,6] data with the ORNL data. Onset of tertiary creep was differentiated from the end of Type I creep through the classification procedure described later in this report.

CLASSIFICATION OF CREEP CURVES

The nonclassical curve depicted in Figure 2 is only one of several types of curves displayed by the current data. That type of curve, displaying both Type I and Type II linear portions, has been denoted as "Intermediate-2" (I2). Some curves showed an initial Type I portion and an apparent transition to the Type II stage, but never regained linearity, possibly because the onset of tertiary creep occurred before the second linear stage was fully established. For purposes of the current analysis, these curves have been denoted as "Intermediate-1" (I1).

There are also many classical creep curves, although these have again been divided into two types. Curves in which Type I creep dominates throughout until the onset of tertiary creep have been denoted "Classical-1" (C1), while curves in which Type II creep dominates throughout have been denoted "Classical-2" (C2). The distinction between these two types of classical curves was based on two criteria. Figure 4 shows the well-known Monkman-Grant relationship for the current data. The data from the classical curves fall into two distinct bands, corresponding to those obtained for the two separate linear creep rates in the I2 creep curves. Also, the strain to the onset of tertiary creep for I2 and C2 curves fell into a band higher than those strains for the type C1 curves.

The class (I1, I2, C1, or C2) of each of the available curves was determined. Taking the class I2 curve as a basic starting point, several trends can be observed. First, postweld heat treatment (PWHT) tends to reduce the amount of Type I creep, making Type II more dominant for the PWHT data than for the annealed data. Type I creep becomes more dominant at higher stresses and lower temperatures. At high stresses the onset of tertiary creep may tend to precede the onset of Type II creep. The onset of Type II creep (being perhaps a precipitation-controlled phenomenon) is strongly temperature dependent and occurs much more slowly at lower temperatures. In summary, the progression appears to be from C1 to I1 to I2 to C2 as the stress is lowered at a given temperature, indicating a gradual increase in the importance of Type II creep. Also, PWHT increases the relative importance of Type II creep. Thus, for most design applications, Type II creep appears to be the more important. Figure 5 schematically illustrates thses types of curves.

Finally, it should be realized that the above classification of creep curves is merely an analytical convenience and is somewhat artificial. The material does not display four distinctly different types of curves. Rather, these distinctions have been made to identify the relative importance of different effects for a given curve.

VARIATIONS IN CREEP STRENGTH

The effect of VAR and ESR melting on mechanical behavior was briefly discussed in Ref. [7], where it was found that VAR and ESR material appeared to have slightly lower creep and tensile strength properties than air-melted material. The effects of heat treatment are larger than those due to melting practice. Figures 6 and 7 compare the ultimate tensile strength and 10^3-hr rupture strength values for various heat treatments with estimated average and minimum values from Ref. [8]. The analyses in Ref. [8] included air-melted annealed and isothermally annealed material only (no PWHT).

Clearly, heat treatment has a significant effect on strength. A heat of average strength in the annealed condition can display roughly minimum strength in the postweld heat treated condition.

Strength variations arise from several sources, including chemical composition, melting practice, processing history, heat treatment, and inherent random scatter in experimental measurement. Metallurgical causes of these variations have been discussed by Klueh [2,3,4]. The goal of the current investigation was to develop a model to describe trends due to systematic effects and to predict behavior in the midrange of the random variations.

ANALYTICAL APPROACH

Two previous analyses of the creep strain-time behavior have been attempted, and their results will be compared with the current results below. However, those analyses, by Hobson and Hebble [8] and by Sterling [9], predicted only classical curve shapes and did not attempt to predict creep strength variations due to factors such as heat treatment and melting practice.

After the above qualitative assessment of the creep behavior of 2 1/4 Cr-1 Mo steel, the following approach was taken here to quantitatively model this behavior. The class C1 curves and the first primary and steady-state portions of the I1 and I2 curves were used as data to model Type I creep. The C2 curves and the second steady-state region of the I2 curves were used to model Type II creep. Both these analyses were then performed in a manner somewhat similar to the Hobson approach, as will be described below.

CHOICE OF EQUATION FORM

On the basis of the results of Hobson [8] for 2 1/4 Cr-1 Mo steel and on various other analyses for other materials [10-13] the classical creep curves and Type I portions of the I1 and I2 curves were fit by the simple rational polynomial creep equation, which was found to yield good fits. The equation used is equivalent to that used by Hobson, although here it has been expressed in the form

$$e_c = Cpt/(1 + pt) + \dot{e}_m t \ , \qquad (1)$$

where

e_c is the creep strain,

t the time

$\dot{e}_m$ is the minimum creep rate,

C is now the limiting value of the transient primary term,

p is the parameter related to the sharpness of the curvature of the primary creep region.

Figure 8 summarizes the properties of the equation, which are described in detail elsewhere [14].

STRESS AND TEMPERATURE DEPENDENCE

The approach taken to evaluate the stress and temperature dependence of the current creep equation was similar to that used by Hobson [8,14]. First, individual curves were fitted to Eq. (10) by the semigraphical technique first proposed by Bunatyan [15] and as recently used by Booker [13]. Again, the initial primary and steady-state stages of C1, I1, and I2 curves were used to determine the parameters C, p, and $\dot{e}_m$ for Type 1 creep (denoted by unprimed symbols); C', p', and $\dot{e}'_m$ were determined from C2 creep curves. In addition, the slope of the second steady-state region for the I2 curves was graphically measured to yield additional values for $\dot{e}'_m$.

The resultant values of C, p, $\dot{e}_m$, C', p', and $\dot{e}'_m$ were then subjected to a least squares regression analysis [16]. The final equations selected to describe the stress and temperature dependence of the creep behavior of 2 1/4 Cr-1 Mo steel were as follows. Type I Creep:

$$\log p = 7.6026 + 3.3396 \log \sigma - 12323/T \;, \tag{2}$$

$$\log C = 1.0328 + 168680/TU - 0.023772U + 0.0079141U \log \sigma \;, \tag{3}$$

$$\log \dot{e}_m = 6.7475 + 0.011426\sigma + (987.72/U)\log \sigma - 13494/T \;, \tag{4}$$

Type II Creep:

$$\log p' = 8.1242 + 0.017678\sigma + (404.63/U)\log \sigma - 11659/T \;, \tag{5}$$

$$\log C' = -0.051086 + 140730/TU - 0.01U + 0.0037345U \log \sigma \;, \tag{6}$$

$$\log \dot{e}'_m = 11.498 - 8.2226U/T - 20448/T + (5862.4/T)\log \sigma \;. \tag{7}$$

In addition, the rupture life (t_r) was described by the following equation:

$$\log t_r = -12.791 - 3.1104\sigma/U - 3.4235 \log(\sigma/U) + 12750/T \;. \tag{8}$$

In Eqs. (2-8), σ is the stress in MPa and T is the temperature in K. The parameter U is the ultimate tensile strength at temperature for a given heat and heat treatment of material, obtained at a strain rate of

6.7×10^{-4}/sec. The inclusion of the ultimate tensile strength terms greatly reduces the uncertainty caused in predictions by the large variations in strength that can be found in different heats and heat treatments of this material. The use of such a term is consistent with the observations of the Hobson analysis. (Hobson used room-temperature ultimate tensile strength rather than elevated-temperature strength, but this usage was primarily due to considerations of data availability.) Previous work [11,12,17] on austenitic stainless steels has also indicated the effectiveness of ultimate tensile strength in predicting creep strength. Table III compares the results obtained by fitting the above equations to the available data with those obtained by using the familiar Larson-Miller [18] parameter. The current equations generally yield superior results, primarily because of the influence of the ultimate tensile strength terms. Figures 9-11 compare predictions for rupture life and minimum creep rate with available data.

The use of the parameters C, p, $\dot{\varepsilon}_m$, C', p', and $\dot{\varepsilon}'_m$ to predict creep behavior will be described in the next section. The rupture life, t_r, is not directly used in predicting strain-time response, although it is a useful piece of information. Moreover, the rupture life can be used indirectly to estimate the time to the onset of tertiary creep for many materials. The nonclassical behavior of 2 1/4 Cr-1 Mo steel makes such evaluation more complicated, but if one defines tertiary creep as an onset of failure, the "true onset of tertiary creep," as described above, occurs at a time t_3 given by [2]

$$t_3 = 0.489 t_r^{1.016} .$$

Or essentially t_3 is half the rupture life.

EVALUATION OF THE EQUATION

Having developed the above equations for the various parameters that describe the creep behavior of 2 1/4 Cr-1 Mo steel, one is still faced with the difficult problem of transforming this information into a unified, consistent predictive system. Some guidance for the actual use of the equation is given in this section. However, the development of a complete constitutive theory for the prediction of behavior in real design situations (variable loads and temperatures, complex states of stress) is beyond the scope of this report. Existing interim constitutive rules for this material are given in Ref. [19].

The most obvious question about the application of the current equations concerns when to use the Type I predictions and when to use the Type II predictions. As a first approach to this problem, the time to the end of the first steady state stage in the I1 and I2 curves (t_I) was determined from each of the available tests by a 0.2% strain offset method. This time can be viewed as the time to the end of Type I creep. All the data for t_I came from tests conducted at 510 and 566°C (950 and 1050°F), since all curves at 454°C (850°F) were classical. This observation is not taken to indicate that the change from Type I to Type II creep does not occur at lower temperatures. This change may well occur at lower stresses than those at which the available tests were run. Analysis of the data for t_I yielded the following equation:

$$\log t_I = -11.098 - 4.0951\sigma/U + 11965/T \,, \tag{10}$$

where

σ, T, and U are as before.

Equation (10) describes the available data for t_I; however, it does predict instances of nonclassical creep at 454°C (850°F) where data indicate that no such nonclassical behavior occurs. Examination of a large number of models failed to reveal one that both described the data for t_I accurately and appeared consistent with the low-temperature behavior. This shortcoming is not surprising in view of the complicated phenomenon being modeled and of the extremely limited nature of the data base. Therefore, until more concrete information becomes available, the following interim procedure is recommended. First, use Eq. (10) only for temperatures of 510°C (950°F) and above. Then, for temperatures of 454°C (850°F) and below, set $t_I = t_r$ from Eq. (8). Between these two temperatures, one can interpolate linearly in $1/T$ or can construct a cubic interpolative polynomial to avoid discontinuities in the slope of the t_I - $1/T$ curve at 454°C and 510°C [20].

Thus, having an estimate for the time t_I, we can use it as follows: At zero time, use the equations for Type I creep and continue to do so until the time reaches t_I. When this criterion is reached, switch to the Type II curve beginning at the current value of creep strain by shifting the Type II curve along the time axis until it corresponds with the Type I curve at $t = t_I$. For instance, say the Type I curve has been used until $t = t_I$ and $e_c = e_I$. Now solve the Type II equation for $t = t_c$ corresponding to $e_c = e_I$. Equation (10) can be solved for time as a function of strain as

$$t_c = \frac{e_c p' - C'p' - \dot{e}_m' + \sqrt{(C'p' + \dot{e}_m' - e_c p') + 4e_c p' \dot{e}_m'}}{2p' \dot{e}_m'} \quad . \qquad (11)$$

Subsequently, the creep strain is given by the Type II equation, except that the equation is evaluated at $t' = t - (t_I - t_c)$. Figure 12 illustrates this construction.

An examination of the predictions of the above equation shows that for very weak material and/or very low stresses, the predicted Type II creep rates can be lower than the Type I creep rates, even at temperatures below 482°C (900°F). *This phenomenon is taken as an indication of the* dominance of the Type II mechanism under these conditions. For very weak material (as indicated by ultimate tensile strength), heat treatment or other factors may have eliminated the possibility of Type I creep through precipitation or other processes. At very low stresses, the Type I mechanism may not become operative since it is felt to be due to a type of dynamic strain aging phenomenon [2]. Analytically, this problem could be handled as follows: For the given combination of σ, T, and U, calculate $\dot{e}_m$ and $\dot{e}'_m$. If $\dot{e}'_m$ is less than $\dot{e}_m$, assume classical Type II creep. This treatment may cause yet another analytical "bump" in the predictions of the equation, but is felt to be necessary to yield reasonable predictions in the low strength and low stress region.

In summary, the recommended rules for application of the equation are as follows for a given σ, T, U combination.

1. First compare $\dot{e}_m$ (Type I minimum creep rate) and $\dot{e}'_m$ (Type II minimum creep rate). If $\dot{e}'_m < \dot{e}_m$, the predicted curve is classical; use the predictions for Type II creep only.

2. If, in the above comparison, $\dot{e}_m < \dot{e}'_m$, begin at time zero with the predictions for Type I creep. Then, when the time reaches $t = t_I$

(where t_I is calculated as above) switch to the Type II predictions by the procedure described above.

Evaluation of the equation under conditions of variable stress and temperature is discussed in Ref. [20].

PREDICTIONS OF THE EQUATION

The obvious standard for judging a creep equation is its ability to predict reasonable values for creep strain for a given heat and heat treatment under a given loading condition. In comparing the predictions of the current equation with those of the Hobson and Sterling equations, one must remember that the two latter equations are somewhat more limited in scope than the current equation. Neither of those equations attempts to reflect variations in strength due to heat-to-heat variations or heat treatment effects.

Figure 13 illustrates predictions of the current equation for individual creep curves by all three equations. The superiority of the current equation is obvious, especially in the case of Fig. 13(b) where that equation accurately predicts the observed nonclassical behavior. The major cause of the improved predictions obtained by use of the current equation is the increased flexibility due to the ultimate tensile strength terms in this equation. Figure 14 illustrates this point even more dramatically. Here, two creep curves obtained at the same stress and temperature, but for different heats, melting practices, and heat treatments are compared with the predictions of the three equations. The variations in strength shown between the two curves are extremely large, indicating a need for some means of predicting these variations. The

Sterling and Hobson equations, having been developed from data for air-melted annealed and isothermally annealed material yield reasonable predictions for the test on heat 20017 air-melted annealed material. However, the isothermally annealed and postweld heat-treated material is obviously much weaker than these equations would predict. The current equation predicts both curves extremely well.

ISOCHRONOUS STRESS-STRAIN CURVES

A popular format for the display of creep strain-time behavior is the isochronous stress-strain curve. Various methods exist for the construction of such curves, many of which are summarized in Ref. [21].

The current creep equation can be used to calculate the creep strain accumulated in a given time at a given stress and temperature for material of a given ultimate tensile strength. Thus, given an estimate of the instantaneous strain incurred upon loading, one can develop isochronous stress-strain curves from the equation. This loading strain can be adequately found from monotonic tensile stress-strain curves. For these predictions, we have chosen to use the reference monotonic tensile curves given [1] in ASME Code Case 1592. These curves do not contain a measure of heat-to-heat and heat treatment effects. However, this shortcoming is not serious, since for our purposes it forces all variations in the isochronous curves to be due to variations in creep strength, thus clarifying the magnitude of those variations. Also, for most normal design conditions, the applied stress is well below the yield strength, making variations in tensile flow properties important primarily for upset conditions only. For comparison, isochronous curves have also been constructed from these same monotonic tensile curves in conjunction with the Sterling and Hobson equations. Note that the curves predicted from the Sterling equation are similar to those given in Code Case 1592 as "average isochronous stress-strain curves."

Figure 15 illustrates predicted 10^2 hour and 10^5 hour isochronous stress-strain curves from the current model. Predictions are shown based on average and minimum (lower tolerance limit) values of ultimate tensile strength as derived from the results of Ref. [8] for air-melted annealed or isothermally annealed material. Shown also are the predictions of the Sterling and Hobson equations for average strength annealed air-melted material. Note that typical strength levels for postweld heat treated ESR and VAR material can be quite near the minimum values shown in Figure 15 (see Figs. 6 and 7). Clearly, the minimum strength curves (dashed lines) in Figure 15 indicate significantly lower creep resistance than do the average strength curves, reflecting the importance of factors such as heat treatment and melting practice in determining the creep behavior of 2 1/4 Cr-1 Mo steel.

The effects of the various rules given above for the use of Type I or Type II creep predictions can be clearly seen in the 566°C (1050°F) 100-hr curve for average strength material in Figure 15c. The S-shaped region around 0.2% strain is due to the transition from Class C2 creep (due to $\dot{e}_m' < \dot{e}_m$) to C1 creep as stress increases, since in this region $t_I > 100$ hr. A second transition region is seen around 1.1% strain because t_I drops below 100 hr in this region.

Similar predictions to Figure 15 are shown in Figure 16 for stress-rupture behavior at 510°C (950°F). Here, average, minimum, and maximum ultimate tensile strength values were used to make predictions of rupture behavior that estimate the middle, bottom, and top of the data scatter band respectively.

LIMITATIONS

The above creep equation is analytically valid under the following conditions, although it must be realized that the actual validity of any equation beyond the range of existing data cannot be verified in the absence of a detailed physical theory for the subject process. No such theory exists for the creep of this material.

Stress: $0 < \sigma <$ ultimate tensile strength

Temperature: 371°C (700°F) $\leq T \leq$ 593°C (1100°F)

Time: $0 \leq t \leq$ time to tertiary creep

In addition, the equation is valid for material with ultimate tensile strength in range given in Table IV from the results of Ref. [8]. This restriction is not a strong one, since almost all 2 1/4 Cr-1 Mo steel meeting applicable specifications should fall within these limits.

SUMMARY AND CONCLUSIONS

An analysis of available creep and creep-rupture data for 2 1/4 Cr-1 Mo steel is presented. It includes data for air-melted, vacuum arc remelted (VAR), and electroslag remelted (ESR) material given annealing or isothermal annealing heat treatments with and without subsequent simulated postweld heat treatments.

The 2 1/4 Cr-1 Mo steel displays two apparently different creep mechanisms, labeled here at Type I and Type II creep. Each type of creep can be described by a single rational polynomial creep equation of the form

$$e_c = \frac{Cpt}{1 + pt} + \dot{e}_m t \ , \qquad (1)$$

where

e_c = the creep strain,

t = the time.

The parameters C, p, and e_m have been expressed as functions of stress, temperature, and ultimate tensile strength at temperature for a given heat and heat treatment of material (these functions are different for the two types of creep). Rules are given above concerning the regions of applicability of Type I and Type II creep.

The rupture life, t_r, was modeled in a fashion similar to the parameters C, p, and e_m above, while the time to tertiary creep was found to be about half the rupture life. Evidence of early onset of tertiary creep in this material appears to be merely a manifestation of a transition from Type I to Type II creep.

Specific conclusions are listed below:

1. Variations in the creep strength of 2 1/4 Cr-1 Mo steel due to melting practice and heat treatment can be large. In general, VAR and ESR material appears slightly weaker than air-melted material. A four hour postweld heat treatment of ESR or VAR material can reduce a heat of approximately average strength to approximately minimum strength as given by the statistical results of Ref. [8].

2. This material has a strong tendency to exhibit nonclassical creep behavior because two separate creep mechanisms exist. The current equation appears to model this nonclassical behavior accurately, but much more information about the metallurgical factors involved in this behavior is needed. Also, the available data fall in a relatively high stress-short time regime in comparison with the range of design interest.

3. Inclusion of ultimate tensile strength terms in the creep and creep rupture models appears to adequately reflect the variations in creep behavior among different heats, melting practices, and heat treatments (annealed or isothermally annealed) with or without subsequent postweld heat treatment. However, such variations can be complex. Full verification of this approach probably awaits both the existence of more long-time data and a better fundamental understanding of this material, including effects of long-term exposure both on the creep strength and on the ultimate tensile strength.

ACKNOWLEDGEMENTS

The author would like to thank R. L. Klueh of ORNL and H. P. Offer and P. J. Ring of the General Electric Company for supplying the data analyzed in this paper. Additional thanks go to Dr. Klueh, R. G. Berggren, C. R. Brinkman, and G. M. Slaughter for reviewing the contents of the paper. Finally, thanks go to ____________ for preparing the manuscript.

REFERENCES

1. Interpretations of the ASME Boiler and Pressure Vessel Code, Case 1592, American Society of Mechanical Engineers, New York, 1974.

2. R. L. Klueh, Creep and Rupture Behavior of Annealed 2 1/4 Cr-1 Mo Steel, ORNL-5219 (December 1976).

3. R. L. Klueh, "Some Observations on the Tertiary Creep Behavior of Annealed 2 1/4 Cr-1 Mo Steel", Proceedings of the Second International Conference on Mechanical Behavior of Materials, American Society for Metals, Metals Park, Ohio, 1975, pp. 434-438.

4. R. L. Klueh, Heat Treatment Effects on the Tensile Properties of Annealed 2 1/4 Cr-1 Mo Steel, ORNL-5144 (May 1976).

5. H. P. Offer, "Metallurgical Characterization of VAR and ESR 2 1/4 Cr-1 Mo Steel", Mechanical Properties Test Data for Structural Materials Quarterly Progress Report, January 31, 1976, ORNL-5112, pp. 304-350.

6. H. P. Offer, "Metallurgical Characterization of VAR and ESR 2 1/4 Cr-1 Mo Steel", Mechanical Properties Test Data for Structural Materials Quarterly Progress Report, July 31, 1976, ORNL-5200, pp. 459-488.

7. H. P. Offer, "Structure and Properties of VAR and ESR 2 1/4 Cr-1 Mo Steel for Nuclear Steam Systems - A Summary", Proc. Second International Conference on Mechanical Behavior of Materials, American Society for Metals, Metals Park, Ohio, 1976, pp. 1775-1779.

8. M. K. Booker, et al., Mechanical Property Correlations for 2 1/4 Cr-1 Mo Steel in Support of Nuclear Reactor Systems Design, ORNL/TM-5329 (June 1976).

9. S. A. Sterling, A Temperature-Dependent Power Law for Monotonic Creep, GA - A13027 (Rev.), June 1974, Revised March 1976.

10. M. K. Booker and V. K. Sikka, Empirical Relationships Among Creep Properties of Four Elevated - Temperature Structural Materials, ORNL/TM-5399, June 1976.

11. M. K. Booker and V. K. Sikka, Analysis of the Creep Strain-Time Behavior of Type 304 Stainless Steel, ORNL-5190, October 1976.

12. W. E. Stillman and V. K. Sikka, "Mathematical Description of the Creep Strain-Time Behavior of Type 316 Stainless Steel", Proc. Second International Conference on Mechanical Behavior of Materials, American Society for Metals, Metals Park, Ohio, 1976, pp. 424-428.

13. M. K. Booker, Mathematical Description of the Elevated Temperature Creep Behavior of Type 304 Austenitic Stainless Steel, in preparation.

14. D. O. Hobson and M. K. Booker, Materials Applications and Mathematical Properties of the Rational Polynomial Creep Equation, ORNL-5202 (December 1976).

15. L. A. Bunatyan, in Proceedings of a Seminar on the Strength of Engineering Components, Izd. Akad. Nauk. SSSR, 1 (2), 1953, as cited in I. A. Oding, ed., Creep and Stress Relaxation in Metals, transl. by E. Bishop, Oliver and Boyd, London, 1959.

16. M. K. Booker, "Regression Analysis of Creep - Rupture Data: A Practical Approach", in preparation.

17. V. K. Sikka, M. K. Booker, and C. R. Brinkman, Use of Ultimate Tensile Strength to Correlate and Predict Creep and Creep Rupture Behavior of Types 304 and 316 Stainless Steel, in preparation.

18. F. R. Larson and J. Miller, "Time-Temperature Relationship for Rupture and Creep Stresses", Trans. Am. Soc. Mech. Eng., 74, 765-75 (July 1952).

19. C. E. Pugh, et al., Background Information for Interim Methods of Inelastic Analysis for High-Temperature Reactor Components of 2 1/4 Cr-1 Mo Steel, ORNL/TM-5226 (May 1976).

20. M. K. Booker, An Interim Analysis of the Creep Strain-Time Characteristics of Annealed and Isothermally Annealed 2 1/4 Cr-1 Mo Steel, in preparation.

21. A. O. Schaefer, ed., The Generation of Isochronous Stress-Strain Curves, American Society of Mechanical Engineers, New York, 1972.

FIGURE CAPTIONS

Fig. 1. Distribution of Available Creep Data for 2 1/4 Cr-1 Mo Steel.

Fig. 2. Schematic Diagrams for Classical (A) and Nonclassical (B) Curves of the Type Observed for 2 1/4 Cr-1 Mo Steel.

Fig. 3. Time to the Onset of Tertiary Creep and Time to the End of Type I Creep as a Function of Rupture Life for Several Heats of 2 1/4 Cr-1 Mo Steel.

Fig. 4. Monkman-Grant Plot for 2 1/4 Cr-1 Mo Steel, Showing Two Distinct Bands for Type I and Type II Linear Creep Rates.

Fig. 5. Schematic Illustration of the Classes of Creep Curves Observed in 2 1/4 Cr-1 Mo Steel. (a) Classical (C1 and C2). (b) Class I1. (c) Class I2.

Fig. 6a. Variation of Ultimate Tensile Strength with Heat Treatment for VAR and ESR 2 1/4 Cr-1 Mo Steel. Average and Minimum Values Derived from Ref. [8] for Air-Melted Annealed Material.

Fig. 6b. Variation of Ultimate Tensile Strength with Heat Treatment for VAR and ESR 2 1/4 Cr-1 Mo Steel. Average and Minimum Values Derived from Ref. [8] for Air-Melted Annealed Material.

Fig. 7a. Variation of 10^3-hr Creep Rupture Strength with Heat Treatment for VAR and ESR 2 1/4 Cr-1 Mo Steel. Average and Minimum Values Derived from Ref. [8] for Air-Melted Annealed Material.

Fig. 7b. Variation of 10^3-hr Creep Rupture Strength with Heat Treatment for VAR and ESR 2 1/4 Cr-1 Mo Steel. Average and Minimum Values Derived from Ref. [8] for Air-Melted Annealed Material.

Fig. 8. Schematic Diagram of the Properties of the Rational Polynomial Creep Equation.

Fig. 9. Relationship Between Ultimate Tensile Strength and 10^3-hr Experimentally Observed Rupture Strength for 2 1/4 Cr-1 Mo Steel, Including Predictions from the Current Model and from that of Ref. [8].

Fig. 10. Type I Minimum Creep Rate at Several Creep Stress Levels as a Function of Ultimate Tensile Strength for 2 1/4 Cr-1 Mo Steel, Including Predictions from the Current Model and from that of Ref. [8].

Fig. 11. Type II Minimum Creep Rate at Several Creep Stress Levels as a Function of Ultimate Tensile Strength for 2 1/4 Cr-1 Mo Steel, Including Predictions from the Current Model and from that of Ref. [8].

Fig. 12. Schematic Illustration of the Recommended Method for Predicting the Transition from Type I to Type II Creep.

Fig. 13. Comparison of Predicted Behavior from the Current Equation, the Sterling Equation, and the Hobson Equation with Actual Experimental Creep Curves. (a) VAR Heat 91506, Heat Treatment ISP; (b) Air-Melted Heat 20017, Heat Treatment IA; (c) VAR Heat 91506, Heat Treatment ANP.

Fig. 14. Comparison of Predicted Behavior from the Current Equation, the Sterling Equation, and the Hobson Equation with Two Actual Experimental Creep Curves Indicating the Magnitude of Possible Variations in Strength. Points Represent Experimental Data for ESR Heat 91505, Heat Treatment ANP and for Air-Melted Heat 20017, Heat Treatment AN-1.

Fig. 15. Predicted Isochronous Stress-Strain Curves from the Current Equation, the Hobson Equation, and the Sterline Equation. Predictions from the Current Equation were made According to the Rules given in the Text. Shown are Predictions for Average and "Minimum" Strength Air-Melted Material (Postweld Heat-Treated Material can Approach the Indicated "Minimum Strength").

Fig. 16. Comparison of Predicted Average, Minimum, and Maximum Strength Stress-Rupture Behavior with Experimental Data.

Table I. Heats of Material Used

Heat	Source	Melting Practice	Content, %								
			C	Mn	Si	Cr	Mo	Ni	S	P	N
20017	ORNL	Air	0.135	0.57	0.37	2.2	0.92	0.16	0.016	0.012	
91505	GE	ESR	0.087	0.47	0.26	2.31	0.99	0.05	0.003	0.007	0.008
30110	GE	ESR	0.1	0.5	0.18	2.26	0.99	0.15	0.007	0.013	0.008
91506	GE	VAR	0.102	0.42	0.32	2.32	1.0	0.06	0.008	0.007	0.009
55262	GE	VAR	0.099	0.5	0.07	2.26	1.0	0.15	0.016	0.013	0.008

Table II. Heat Treatments Used on 2 1/4 Cr-1 Mo Steel

Heat 20017[a]

AN-1: Austenitize 1 hr at 927°C (1700°F); furnace cool.

AN-2: Austenitize 1 hr at 927°C; furnace cool (faster than AN-1).

IA: Austenitize 1 hr at 927°C; furnace cool at about 83°C/hr (150°F/hr) to 704°C (1400°F); hold 2 hr; furnace cool.

Heats R0110 and 55262

ISPP Isothermal Anneal:	954°C (1750°F) for 0.5 hr Furnace cool to 710°C (1310°F); hold 2.5 hr Air cool to room temperature.
Postweld: (PWHT)	727°C (1340°F) for 4 hr. Air cool to room temperature.
ANN Anneal:	916°C (1680°F) for 1.25 hr. Furnace cool [at 27.7-55.6°C/hr (50-100°F/hr) to 316°C (600°F)]. Air cool to room temperature.
ANNP: Same as ANN, plus Postweld:	727°C (1340°F) for 4 hr. Air cool to room temperature.

Heats 91505 and 91506

AN: Austenitize 1 hr at 927°C; furnace cool to 316°C at 56°C/hr max.

ANP: Same as AN plus postweld, 4 hr, 727°C (1340°F).

IS: Austenitize 0.5 hr 927°C; furnace cool to 704°C at 125°C/hr max; hold 1.5 hr.

ISP: Same as M plus postweld, 4 hr, 727°C.

ISP1: Same as M plus postweld, 40 hr, 727°C.

[a]R. L. Klueh, Heat Treatment Effects on the Tensile Properties of Annealed 2 1/4 Cr-1 Mo Steel, ORNL-5144 (October 1975).

Table III. Summary of Fits to Data

Parameter	Number of Data	R^2, Coefficient of Determination,[a] %	
		"Best Model"[b]	Larson-Miller Parameter[c]
		Type I Creep	
C	59	68.56	46.08
p	59	55.22	55.51
$\dot{e}_m$	96	81.71	43.65
		Type II Creep	
C'	25	68.57	49.91
p'	25	83.46	74.27
$\dot{e}'_m$	62	86.31	43.39
t_I	57	74.59	68.63
t_r	121	80.43	49.17

[a]The value of R^2 here gives the percentage of data variations described by the model.

[b]Given in text.

[c]Expressed as $\log y = (\alpha_0 + \alpha_1 \log \sigma + \alpha_2\sigma)/T + \alpha_3$. No models without UTS terms were significantly better than this one.

Table IV. Expected Range of Ultimate Tensile Strength Values for 2 1/4 Cr-1 Mo Steel from Ref. [8].

Temperature		Ultimate Tensile Strength, MPa (ksi)		
(°C)	(°F)	Lower Limit	Expected Value	Upper Limit
20	68	405 (58.7)	508 (73.7)	612 (88.8)
50	122	387 (56.1)	486 (70.5)	586 (85.0)
100	212	363 (52.6)	464 (67.3)	564 (81.8)
150	302	353 (51.2)	455 (66.0)	557 (80.8)
200	392	354 (51.3)	456 (66.1)	558 (80.9)
250	482	362 (52.5)	462 (67.0)	563 (81.7)
300	572	371 (53.8)	469 (68.0)	567 (82.2)
350	662	376 (54.5)	473 (68.6)	570 (82.7)
400	752	371 (53.8)	468 (67.9)	565 (81.9)
450	842	354 (51.3)	452 (65.6)	549 (79.6)
500	932	322 (46.7)	418 (60.6)	515 (74.7)
550	1022	267 (38.7)	364 (52.8)	460 (66.7)
600	1112	181 (26.3)	284 (41.2)	387 (56.1)

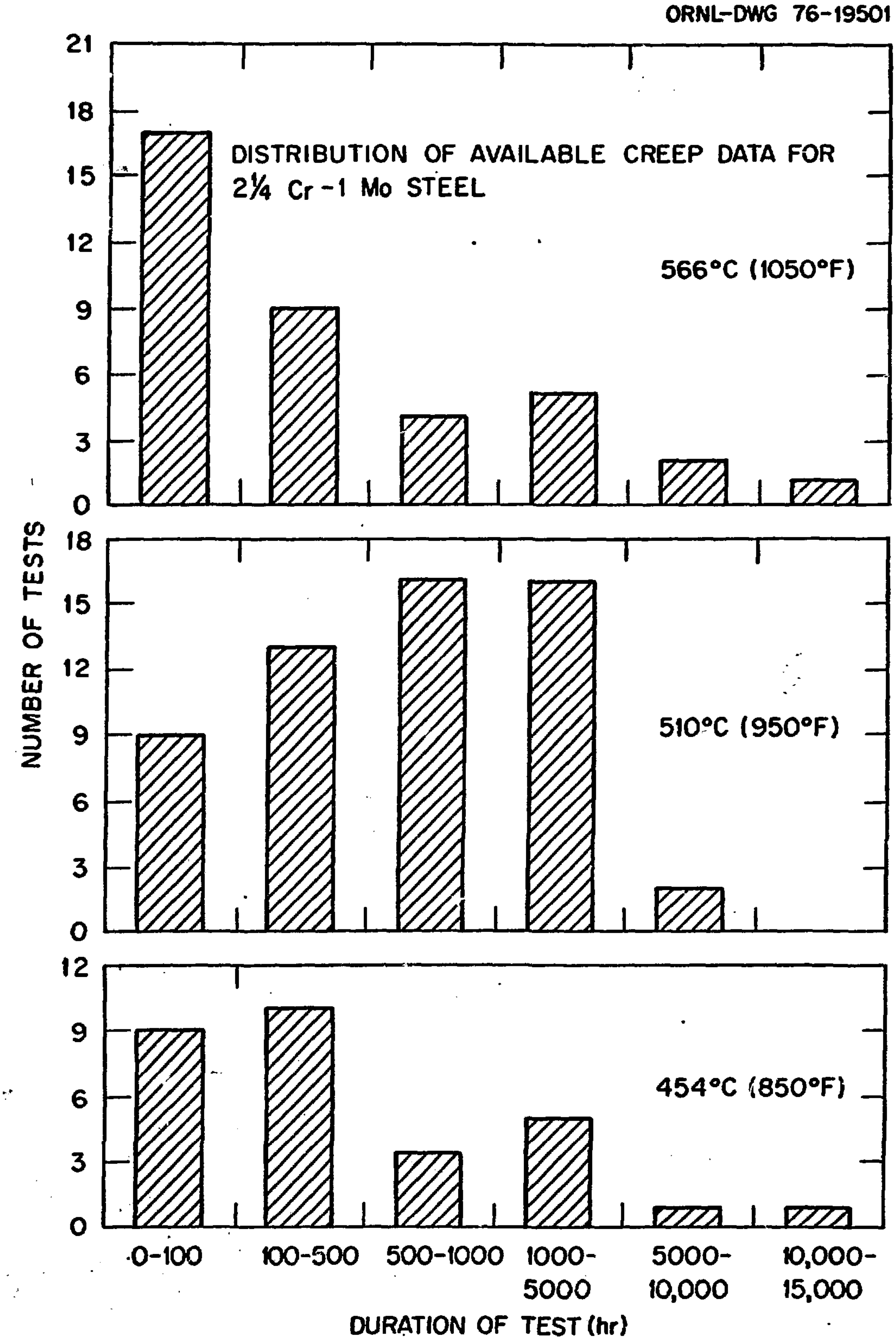

Fig. 1. Distribution of Available Creep Data for 2 1/4 Cr-1 Mo Steel.

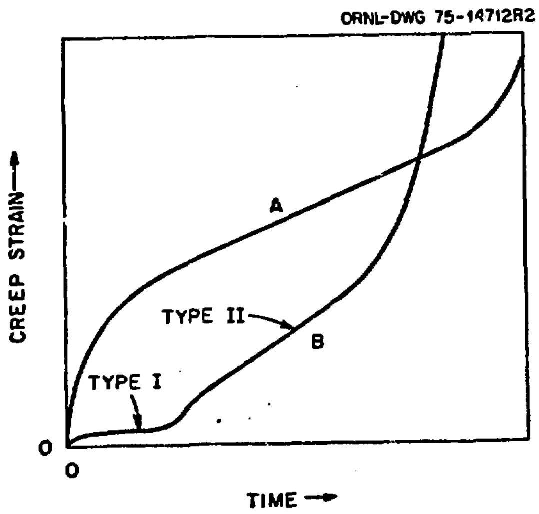

Fig. 2. Schematic Diagrams for Classical (A) and Nonclassical (B) Curves of the Type Observed for 2 1/4 Cr-1 Mo Steel.

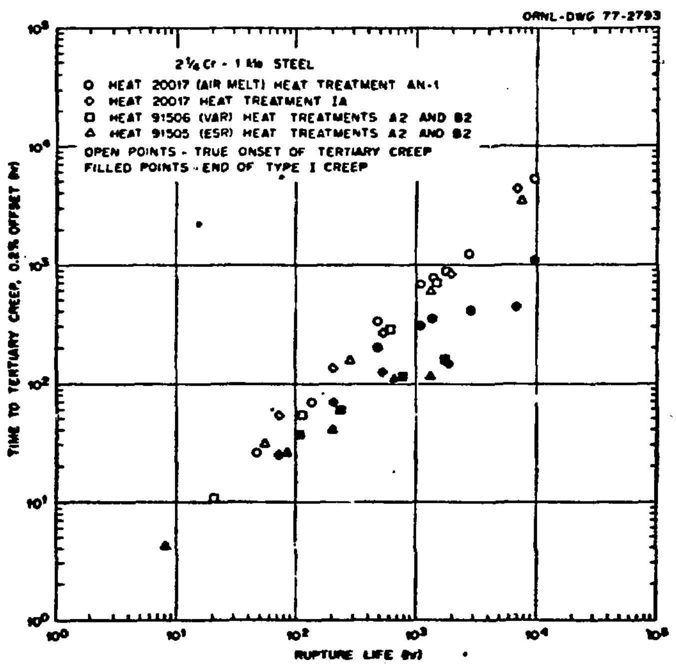

Fig. 3. Time to the Onset of Tertiary Creep and Time to the End of Type I Creep as a Function of Rupture Life for Several Heats of 2 1/4 Cr-1 Mo Steel.

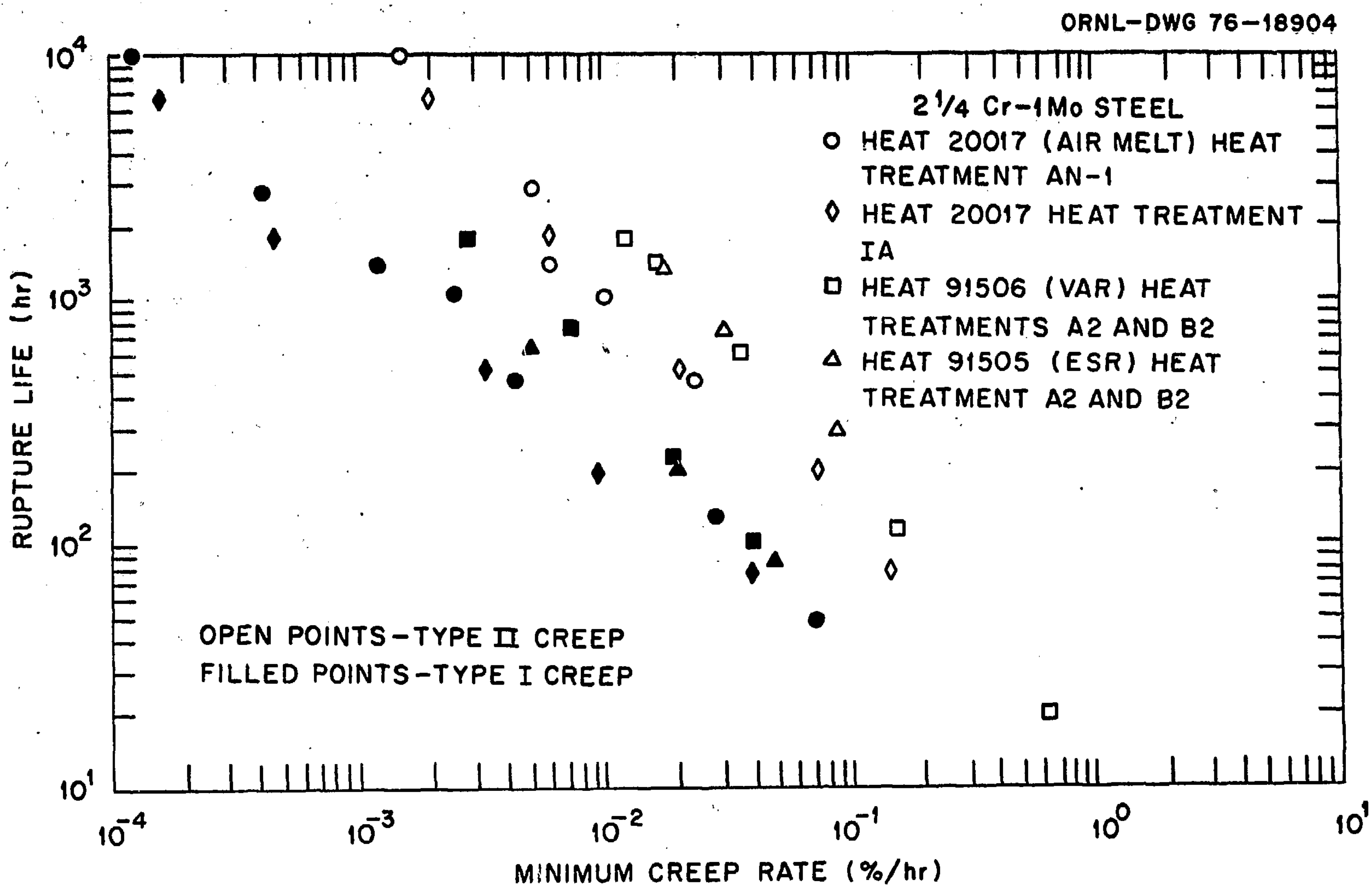

Fig. 4. Monkman-Grant Plot for 2 1/4 Cr-1 Mo Steel, Showing Two Distinct Bands for Type I and Type II Linear Creep Rates.

ORNL-DWG-76-18906

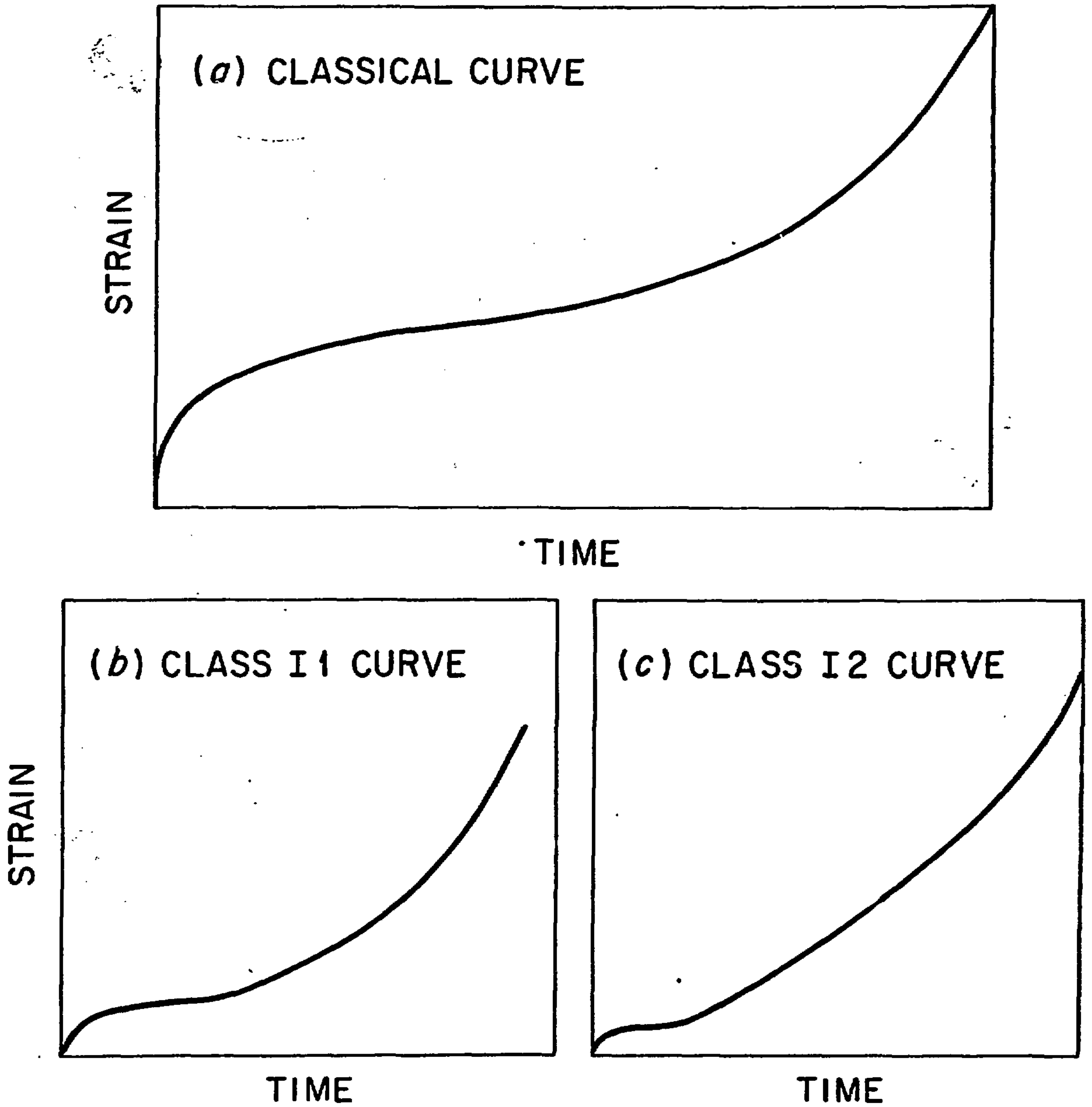

Fig. 5. Schematic Illustration of the Classes of Creep Curves Observed in 2 1/4 Cr-1 Mo Steel. (a) Classical (C1 and C2). (b) Class I1. (c) Class I2.

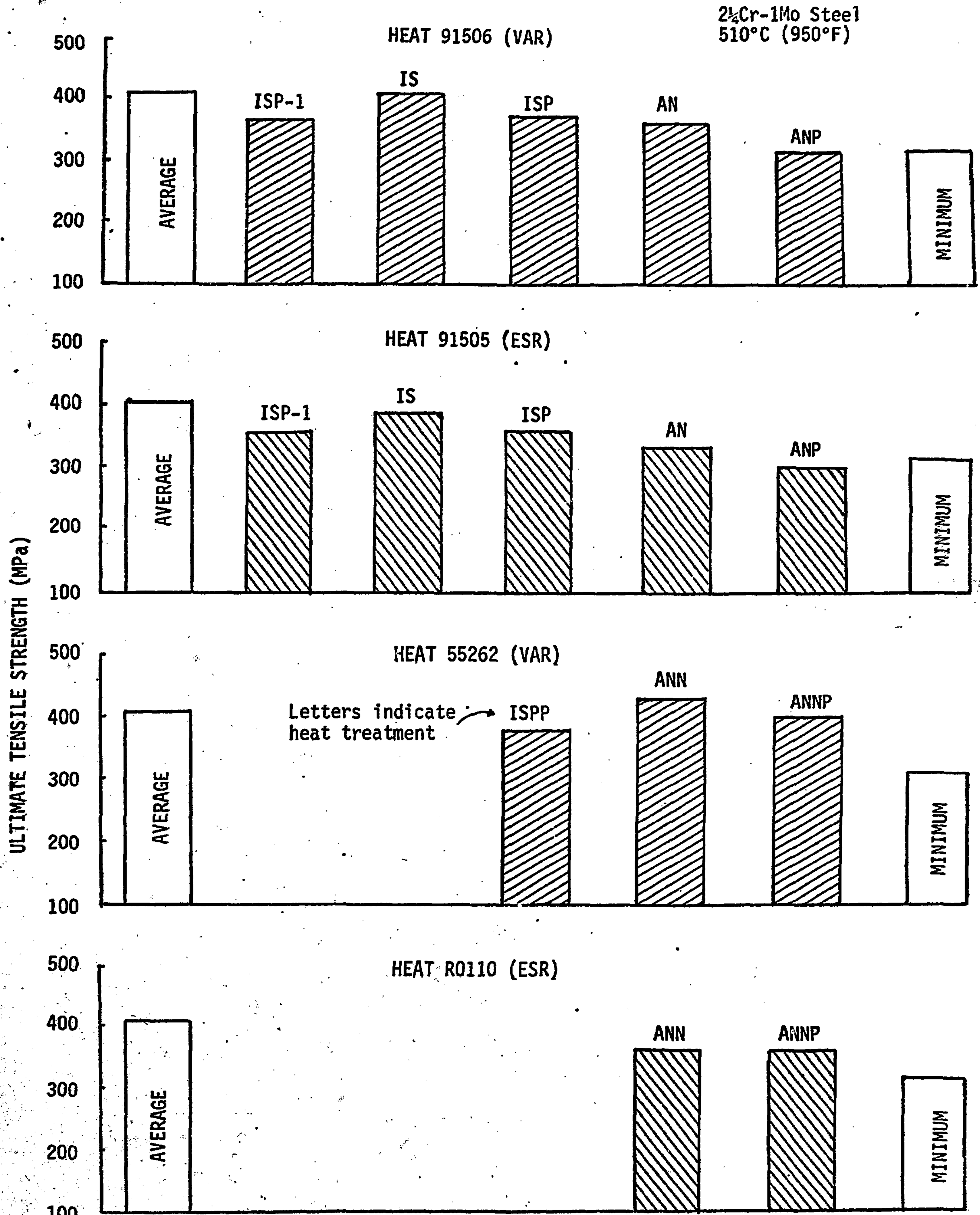

Fig. 6a. Variation of Ultimate Tensile Strength with Heat Treatment for VAR and ESR 2 1/4 Cr-1 Mo Steel. Average and Minimum Values Derived from Ref. [8] for Air-Melted Annealed Material.

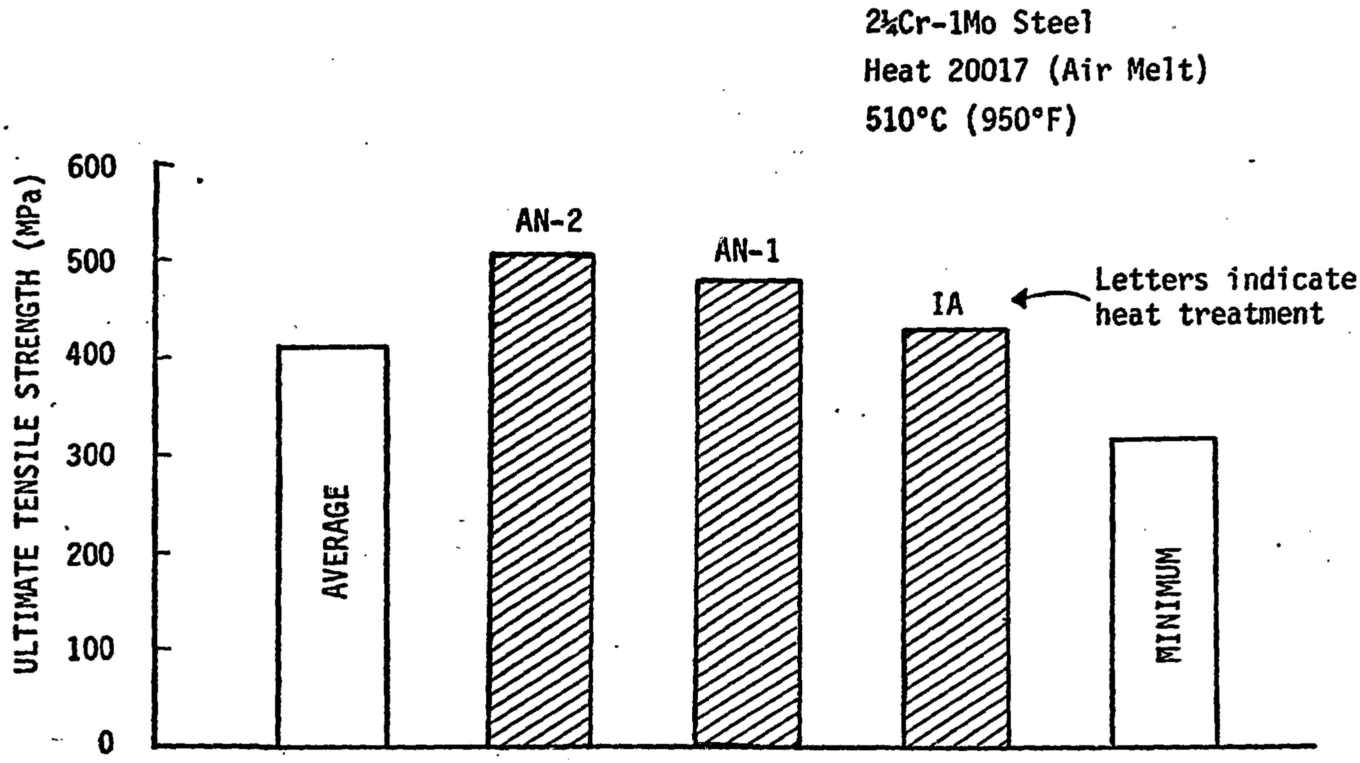

Fig. 6b. Variation of Ultimate Tensile Strength with Heat Treatment for VAR and ESR 2 1/4 Cr-1 Mo Steel. Average and Minimum Values Derived from Ref. [8] for Air-Melted Annealed Material.

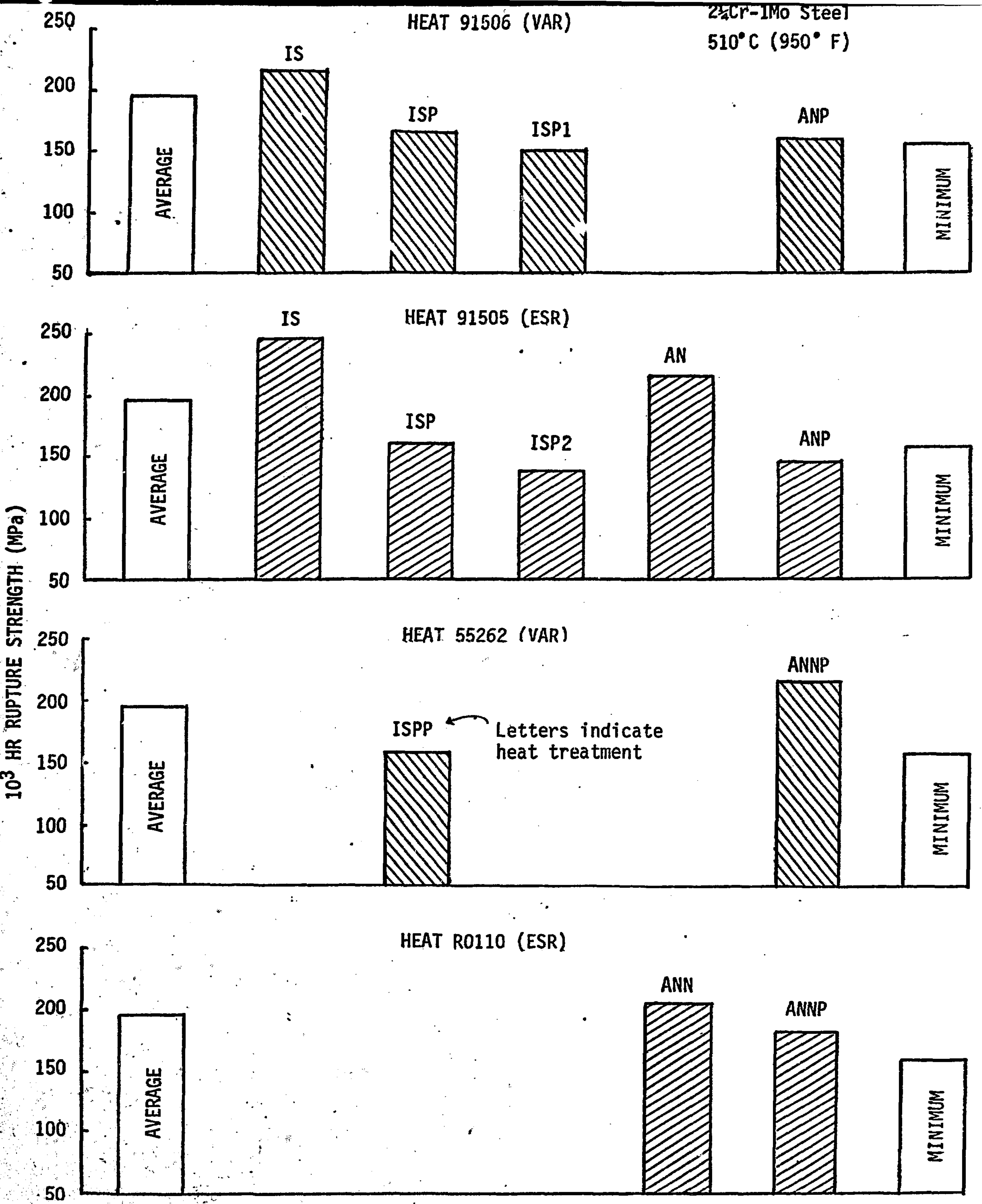

Fig. 7a. Variation of 10^3-hr Creep Rupture Strength with Heat Treatment for VAR and ESR 2 1/4 Cr-1 Mo Steel. Average and Minimum Values Derived from Ref. [8] for Air-Melted Annealed Material.

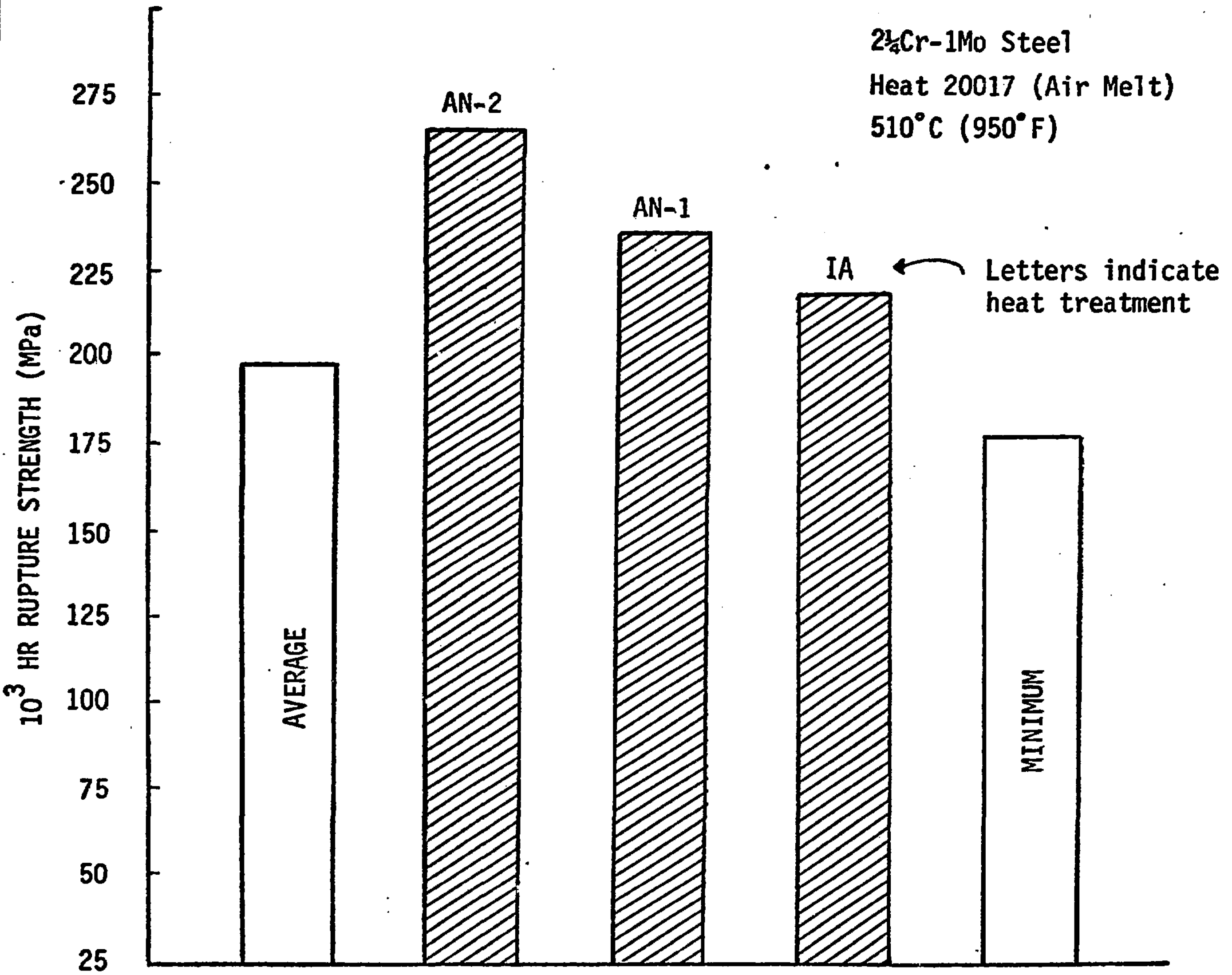

Fig. 7b. Variation of 10^3-hr Creep Rupture Strength with Heat Treatment for VAR and ESR 2 1/4 Cr-1 Mo Steel. Average and Minimum Values Derived from Ref. [8] for Air-Melted Annealed Material.

ORNL-DWG 76-3985R

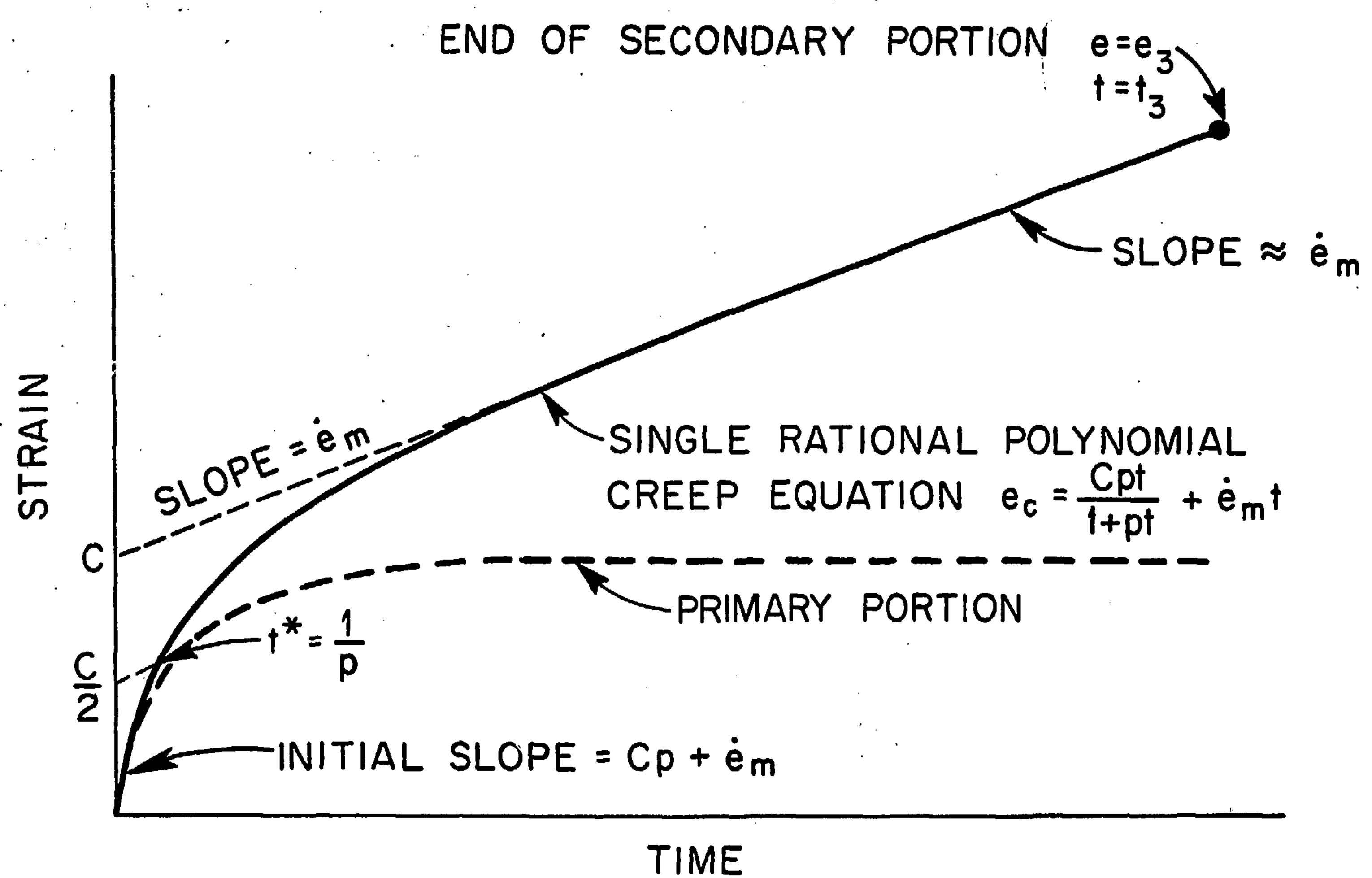

Fig. 8. Schematic Diagram of the Properties of the Rational Polynomial Creep Equation.

ORNL-DWG 76-18903

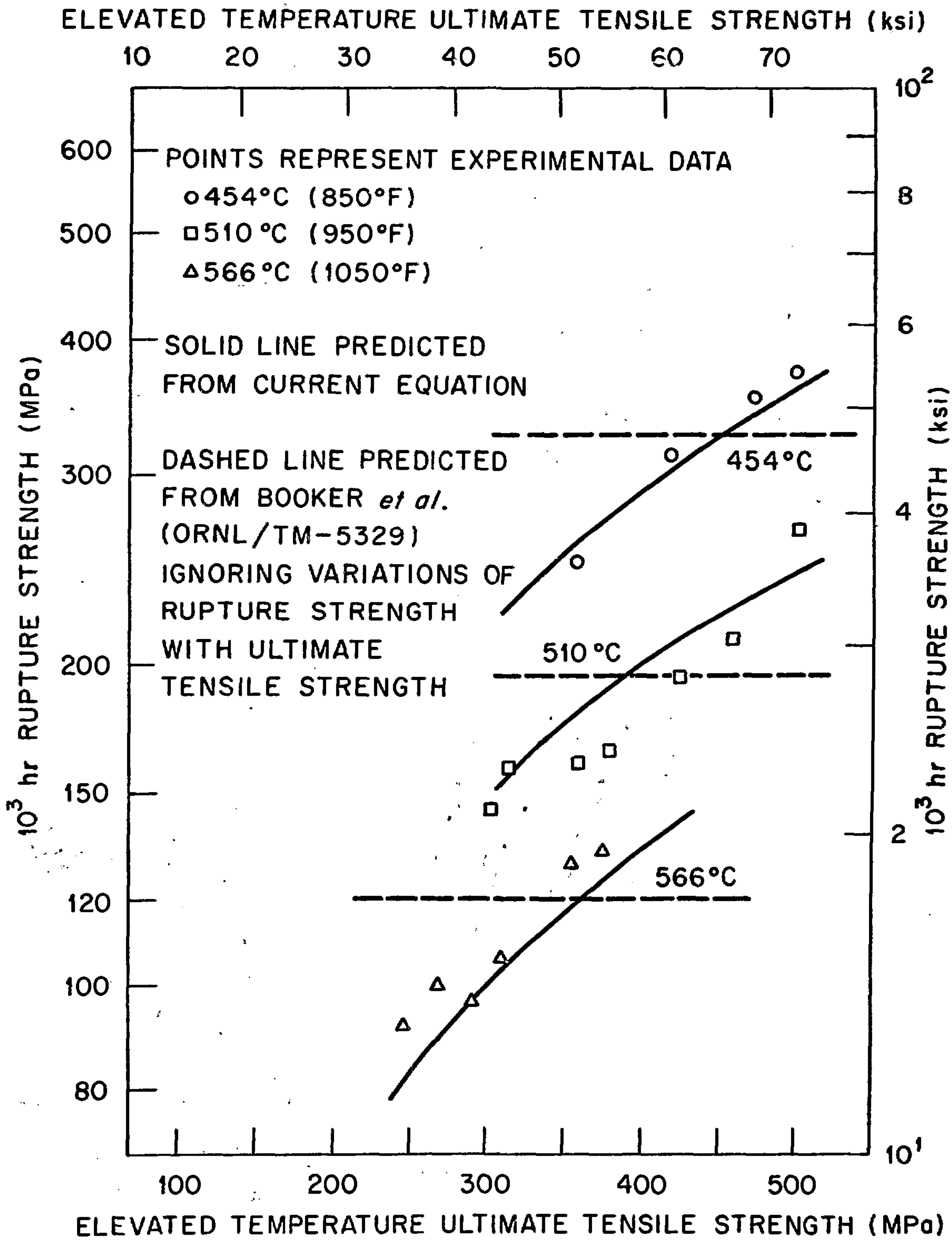

Fig. 9. Relationship Between Ultimate Tensile Strength and 10^3-hr Experimentally Observed Rupture Strength for 2 1/4 Cr-1 Mo Steel, Including Predictions from the Current Model and from that of Ref. [8].

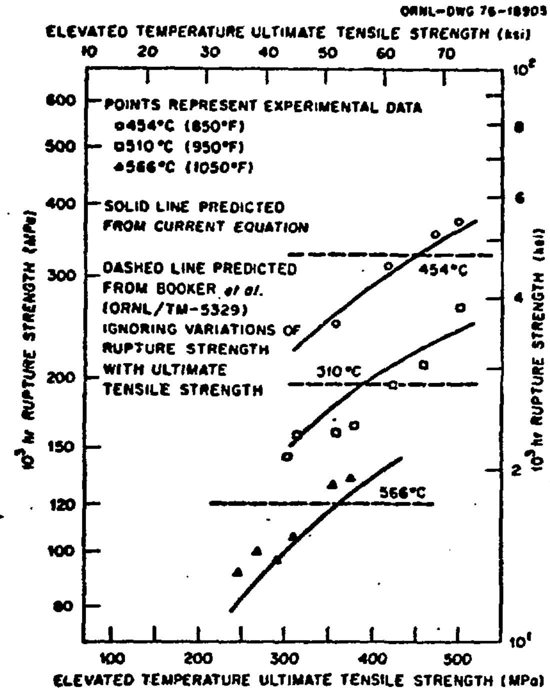

Fig. 10. Type I Minimum Creep Rate at Several Creep Stress Levels as a Function of Ultimate Tensile Strength for 2 1/4 Cr-1 Mo Steel, Including Predictions from the Current Model and from that of Ref. [8].

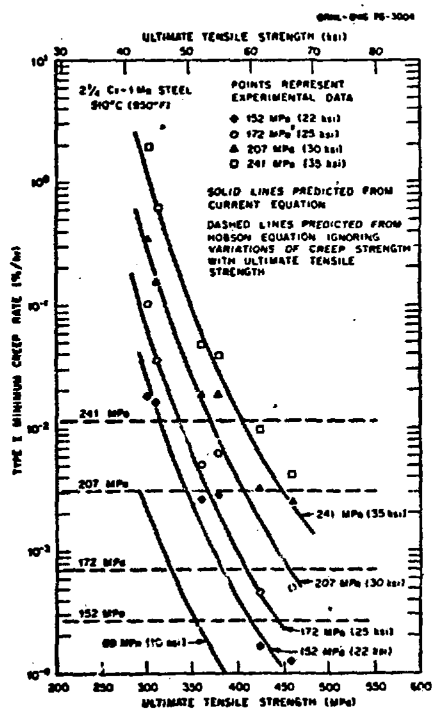

Fig. 11. Type II Minimum Creep Rate at Several Creep Stress Levels as a Function of Ultimate Tensile Strength for 2 1/4 Cr-1 Mo Steel, Including Predictions from the Current Model and from that of Ref. [8].

ORNL-DWG 76-18913

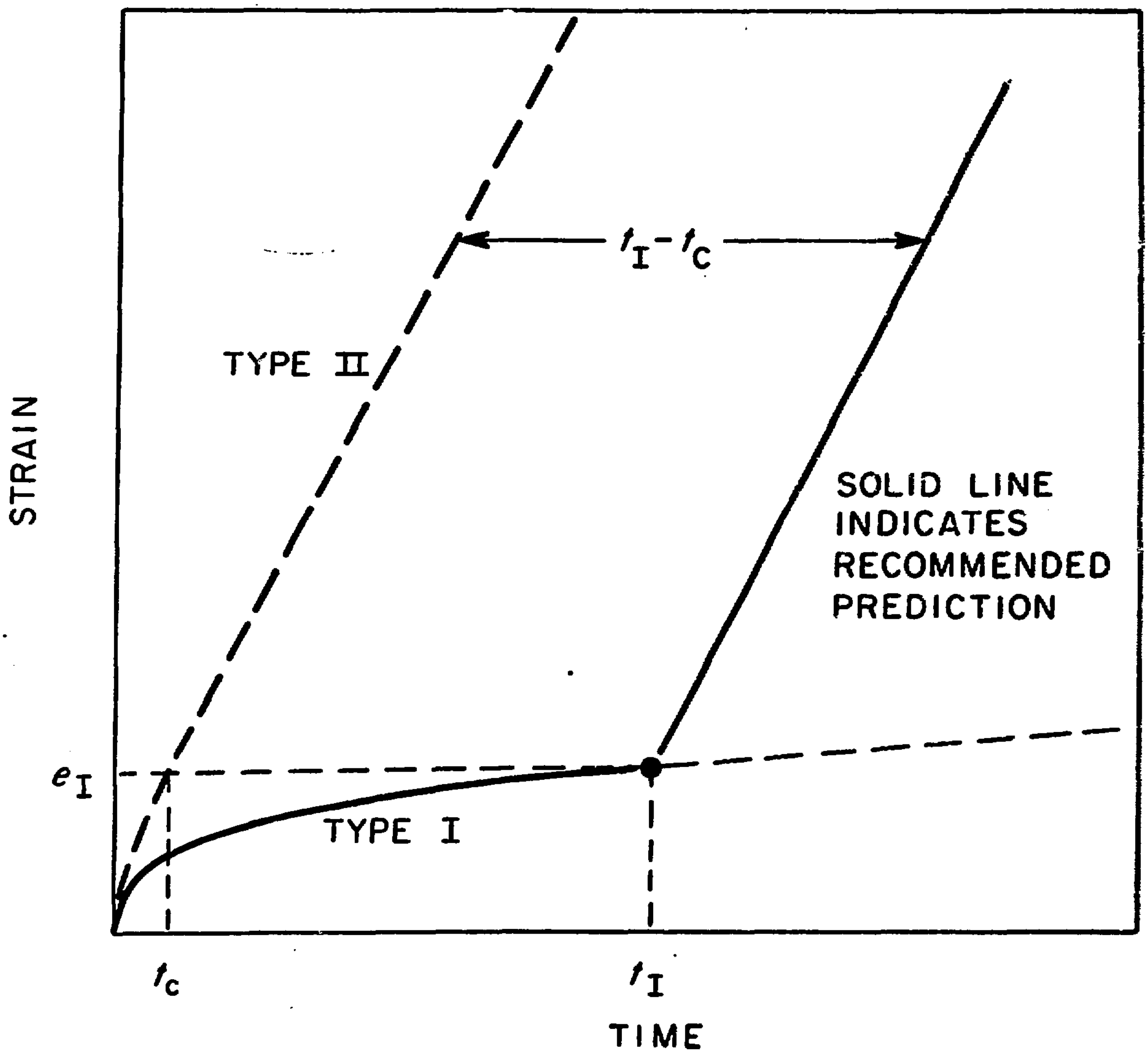

Fig. 12. Schematic Illustration of the Recommended Method for Predicting the Transition from Type I to Type II Creep.

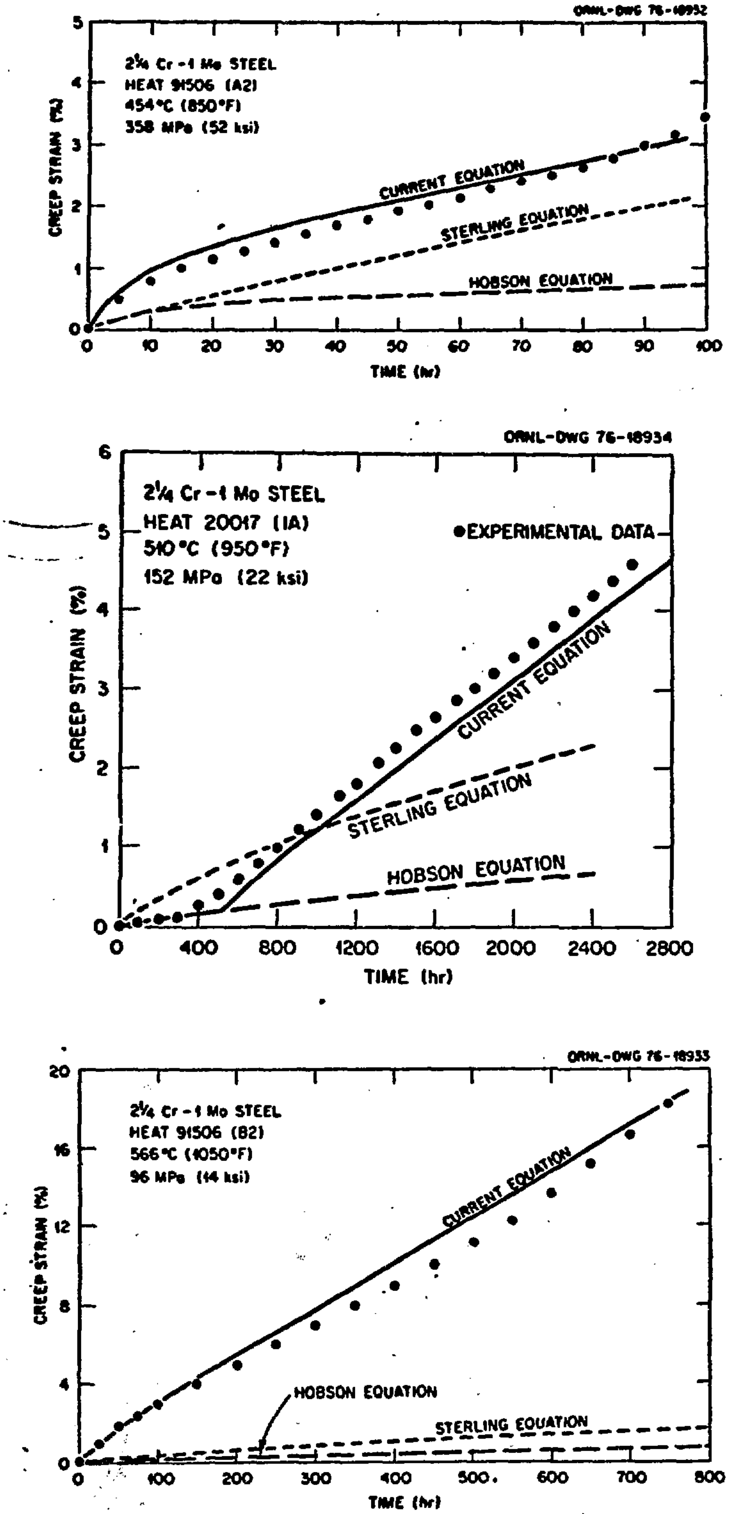

Fig. 13. Comparison of Predicted Behavior from the Current Equation, the Sterling Equation, and the Hobson Equation with Actual Experimental Creep Curves. (a) VAR Heat 91506, Heat Treatment ISP; (b) Air-Melted Heat 20017, Heat Treatment IA; (c) VAR Heat 91506, Heat Treatment ANP.

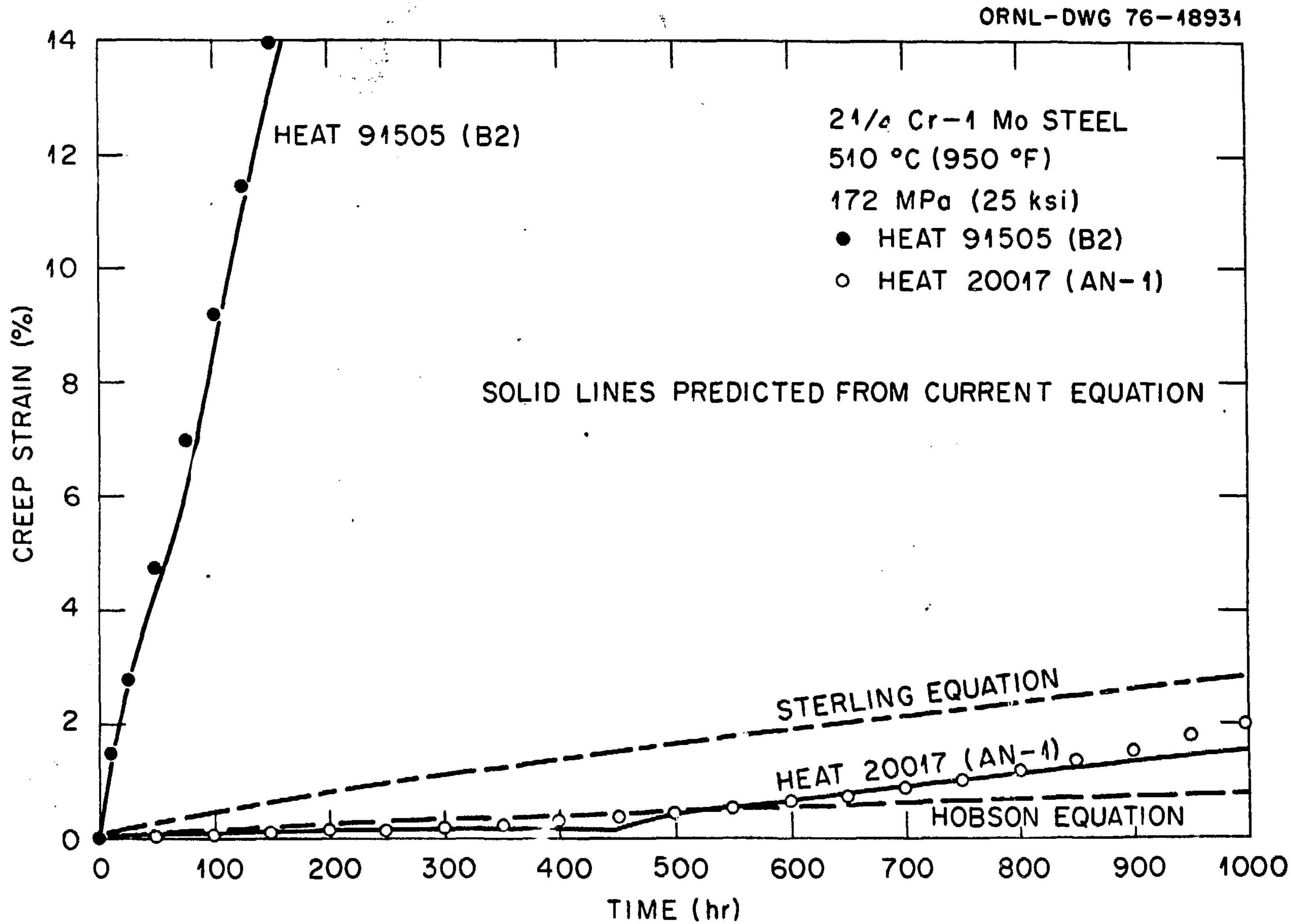

Fig. 14. Comparison of Predicted Behavior from the Current Equation, the Sterling Equation, and the Hobson Equation with Two Actual Experimental Creep Curves Indicating the Magnitude of Possible Variations in Strength. Points Represent Experimental Data for ESR Heat 91505, Heat Treatment ANP and for Air-Melted Heat 20017, Heat Treatment AN-1.

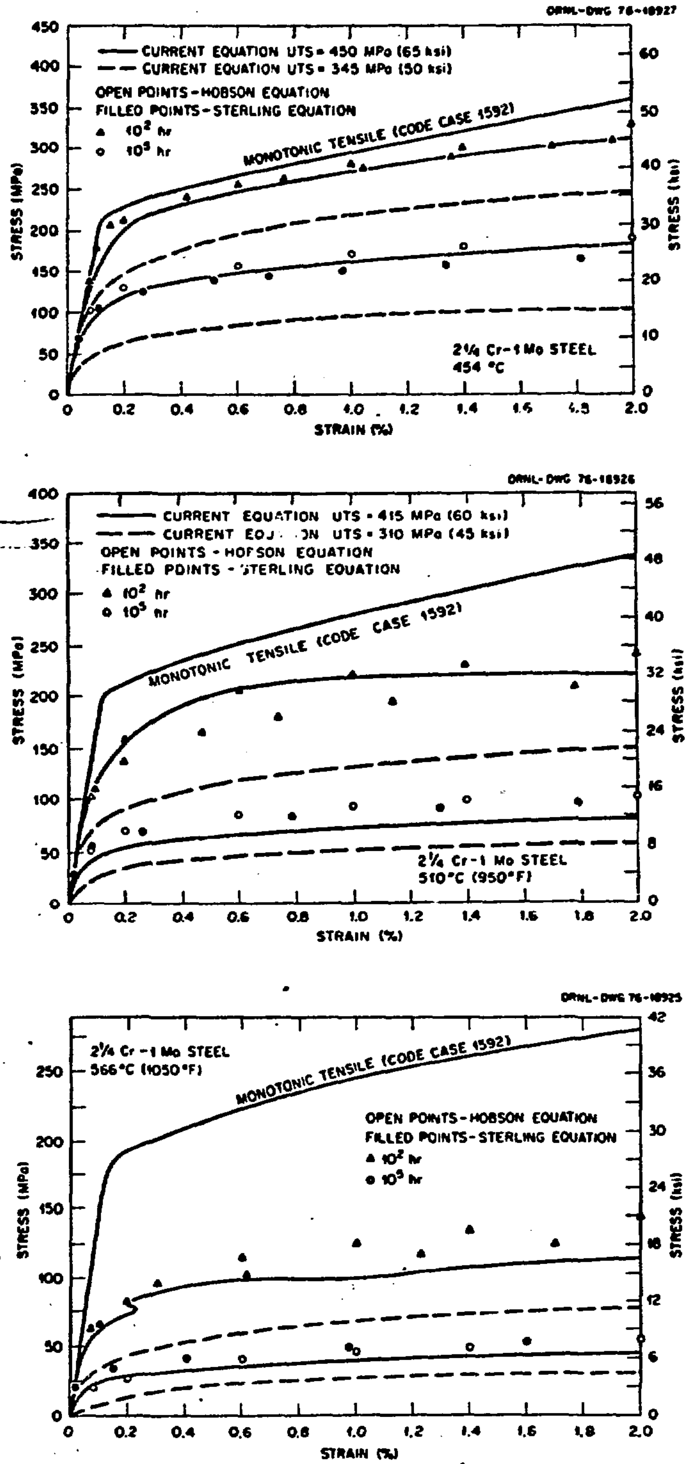

Fig. 15. Predicted Isochronous Stress-Strain Curves from the Current Equation, the Hobson Equation, and the Sterline Equation. Predictions from the Current Equation were made According to the Rules given in the Text. Shown are Predictions for Average and "Minimum" Strength Air-Melted Material (Postweld Heat-Treated Material can Approach the Indicated "Minimum Strength").

ORNL-DWG 77-6200

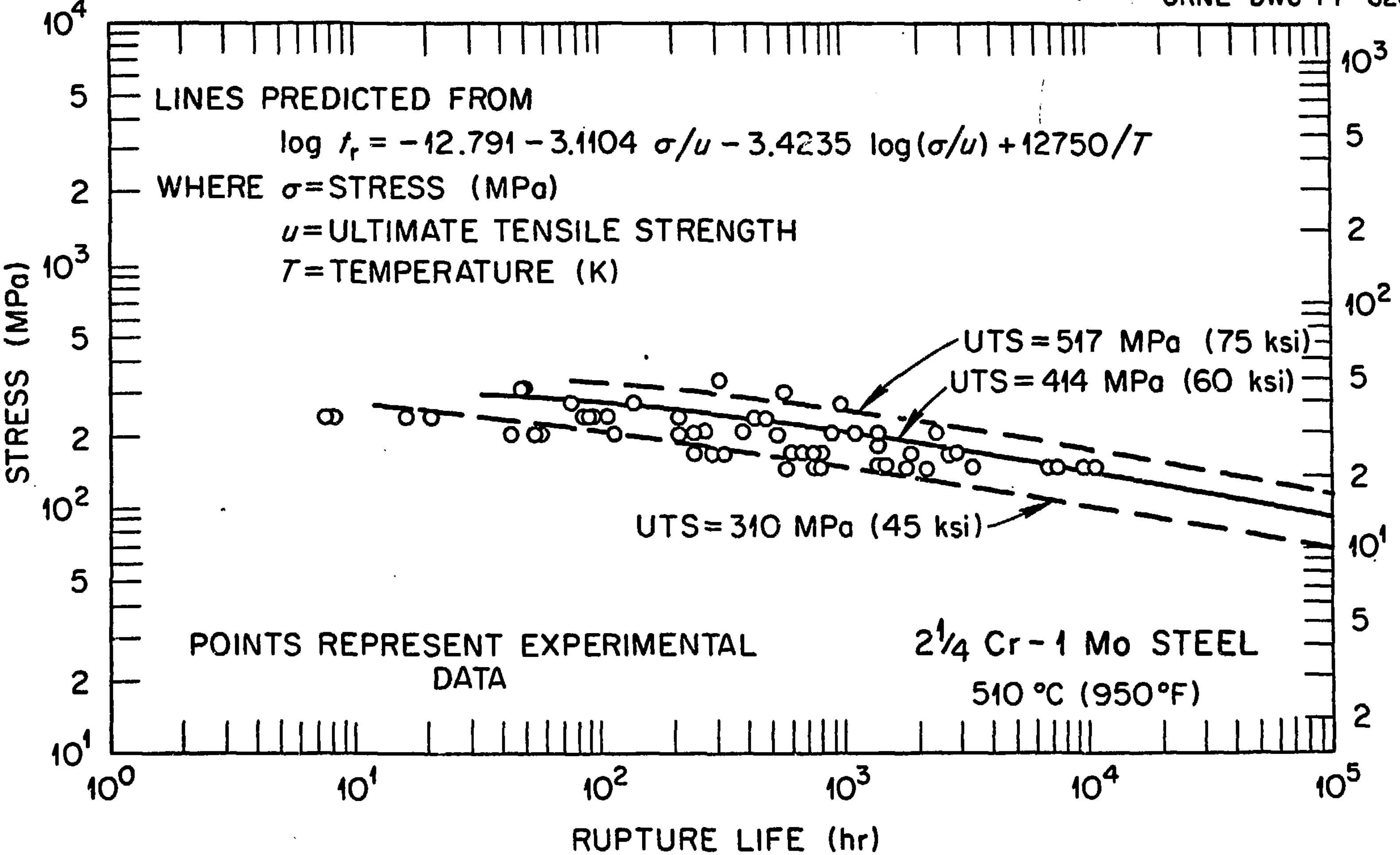

Fig. 16. Comparison of Predicted Average, Minimum, and Maximum Strength Stress-Rupture Behavior with Experimental Data.